Applied Clay Science 153 (2018) 205–216

Contents lists available at ScienceDirect

Applied Clay Science

journal homepage: www.elsevier.com/locate/clay

Research paper

Pyrolysis behaviors of organic matter (OM) with the same alkyl main chain but different functional groups in the presence of clay minerals

Hongmei Liu[a], Peng Yuan[a,*], Dong Liu[a], Hongling Bu[a,b], Hongzhe Song[a,b], Zonghua Qin[c], Hongping He[a]

[a] CAS Key Laboratory of Mineralogy and Metallogeny, Guangdong Provincial Key Laboratory of Mineral Physics and Materials, Guangzhou Institute of Geochemistry, Chinese Academy of Sciences, Guangzhou 510640, China
[b] University of Chinese Academy of Sciences, Beijing 100049, China
[c] State Key Laboratory of Ore Deposit Geochemistry, Institute of Geochemistry, Chinese Academy of Sciences, Guiyang 550002, China

ARTICLE INFO

Keywords:
Organic matter
Clay minerals
Association way
Pyrolysis
Solid acidity

ABSTRACT

Organic matter (OM)-clay mineral complexes, especially OM-clay interlayer complexes, exist widely in soil, sediment, and source rock. These associations can influence the pyrolytic behaviors of OM. In addition, the nature of OM may also affect pyrolysis due to the variety and complexity of the structure and chemical composition of natural organics. In this study, to investigate the influences of the nature of OM as well as the interface association between OM and clay minerals on the pyrolysis of OM, interlayer clay-OM complexes and clay-OM mixtures were prepared and thermogravimetry coupled with Fourier transform infrared spectroscopy (TG-FTIR) was adapted to monitor the pyrolytic temperatures and products of these complexes. A series of OM with the same alkyl main chain but different functional groups, i.e., Lauric acid (LA), Dodecylamine (DA), 12-Aminolauric acid (ALA) and Dodecyl trimethyl ammonium bromide (DTAB), was used, and montmorillonite (Mt) was selected as the representative clay mineral. The results showed that Mt decreased the decomposition temperature of the carboxyl groups that contained OM (LA and ALA), promoted the generation of CO_2 via the catalysis of the Lewis acid sites of Mt, and delayed the decomposition of DA and DTAB. The interlayer Brønsted acid sites allowed the nitrogen-containing organics to undergo Hoffmann elimination. The pyrolytic behaviors of OM within the interlayers of Mt were more strongly affected than those on the external surface of Mt The pyrolytic performance of OM was closely related to the association ways between OM and clay minerals, the nature of clay minerals, and the nature of OM. The interlayer space was shown to be particularly important for the preservation and catalysis of organics.

1. Introduction

The catalytic functions of clay minerals for natural hydrocarbon generation have been well demonstrated in numerous studies (Jurg and Eisma, 1964; Shimoyama and Johns, 1971; Heller-Kallai et al., 1984). The clay minerals of the smectite group, such as montmorillonite (Mt), have received particular attention because of their known catalytic activities and their ubiquity in low-maturity source rocks and sediments. Traditionally, model organic matter (OM), such as kerogen and bitumen that were separated from source rocks, and synthetic organics, such as fatty acids and fatty acid esters, were mixed with clay minerals, and these mixtures were used in pyrolysis experiments to explore the pyrolytic behaviors of organics in the presence of clay minerals (Jurg and Eisma, 1964; Shimoyama and Johns, 1971; Faure et al., 2003; Li et al., 2003; Zhang et al., 2005; Faure et al., 2006). Under this scenario, OM and clay were assumed to exist separately and the catalytic effects of clay minerals were believed to occur merely on the external surface of clay minerals.

However, in the past several decades, this knowledge has been revised based on the findings of the wide existence of clay-OM associations in sedimentary rocks, which have been demonstrated by a variety of independent studies (Bergamaschi et al., 1997; Ransom et al., 1998; Mayer, 1999; Ingalls et al., 2004; Mayer, 2004; Lopez-Sangil and Rovira, 2013; Zhu et al., 2016). These mentioned studies have verified that in many cases, OM in sediments is primarily associated with clay minerals rather than existing alone. This is indicated by observations that it is difficult to separate organic material from clay minerals using physical methods, as well as the direct proportionality between the concentration of organic matter and the sediment surface area (Keil et al., 1994; Mayer, 1994).

* Corresponding author.
E-mail address: yuanpeng@gig.ac.cn (P. Yuan).

https://doi.org/10.1016/j.clay.2017.12.028
Received 27 October 2017; Received in revised form 13 December 2017; Accepted 14 December 2017
Available online 22 December 2017
0169-1317/

Particularly, a special clay-OM association in natural sedimentary environments, i.e., the storage of OM within the interlayer space of layered silicates, has been proposed as early as the 1970s (Theng, 1974) and confirmed by a series of following studies (Perezrodriguez et al., 1977; Theng et al., 1986; Kennedy et al., 2002; Cai et al., 2007). From the perspective of surface chemistry properties of swelling clay minerals, there are a variety of natural polar or charged organics, including ammonium ions, that are chemically similar to the model organics used in this study (He et al., 2005; Xi et al., 2007; Zhu et al., 2009), humic acid (Wang and Huang, 1986), and proteins (Yu et al., 2013), which could be intercalated into the interlayer of swelling clay minerals through cation-exchange reactions. Particularly, once the interlayer space is opened through the intercalation of the above-mentioned organics, more types of organics, including neutral or non-polar molecules that initially cannot enter pristine interlayer sites through cation-exchange, could also be intercalated into interlayer space through interactions, such as hydrophobic interactions with pre-intercalated organics (Lagaly et al., 2013).

The existence of naturally occurring interlayer clay-OM complexes has been demonstrated in a variety of studies in which the interlayer distance of Mt or mixed-layered Mt-illite in source rocks or sediments was found to be expanded due to the intercalation of natural organics (Perezrodriguez et al., 1977; Theng et al., 1986; Schulten et al., 1996; Lu et al., 1999; Kennedy et al., 2002; Cai et al., 2007; Zhu et al., 2016). Theng et al. (1986) reported the occurrence of interlayer clay-organic complexes in the clay fraction of soil samples from Maungatua, New Zealand; the interlayer organics, as revealed by ^{13}C NMR spectroscopic analyses, comprised polymethylene chains containing carboxyl and hydroxyl groups (Theng et al., 1986). Schulten et al. (1996) characterized the organic matter in the interlayer clay-organic complexes from the Maungatua soil using pyrolysis methylation-mass spectrometry (Schulten et al., 1996). Lu et al. (1999) investigated the OM-clay associations in immature source rocks from the Dongying depression of the Bohai Bay Basin, China, and found that the content of the interlayer organics accounted for approximately 25%–50% (mass%) of the total extracted organics (Lu et al., 1999). Kennedy and Wagner (2011) identified the occurrence of OM-clay complexes in Late Cretaceous black shales from the Ocean Drilling Program site 959 of the Deep Ivorian Basin, where OM was located within the interlayer sites of the mixed layer illite-smectite (Kennedy and Wagner, 2011). Recently, Kennedy et al. (2014) further obtained direct high-resolution transmission electron microscopy (HRTEM) evidences of occurrence of OM as nanometer-scale intercalations in swelling clays.

Given the understandings of the OM-clay associations revealed by the abovementioned studies, it is obvious that the roles of clay minerals, especially the swelling clay minerals whose interlayers are able to host OM, in the pyrolysis of OM must be reevaluated. Meanwhile, natural organics with various structures and chemical compositions exhibited different evolutions. For example, three main types of kerogen were identified, from I, starting at low maturity with high H/C and low O/C, to III, starting at low maturity with low H/C and high O/C. It was widely accepted that the type of kerogen largely influenced both the amount and chemical composition of the products generated upon burial (Vandenbroucke and Largeau, 2007). Thus, the nature of OM deserves extra attention in assessing their pyrolytic behaviors in the presence of clay minerals.

In this work, a series of OM-clay complexes were prepared for their use in the pyrolysis experiments of OM. Montmorillonite (Mt) was used as a model clay mineral because of its ubiquity in the source rock and its high expanding capacity. Lauric acid ($CH_3(CH_2)_{10}COOH$, hereafter denoted as LA), Dodecyl amine ($CH_3(CH_2)_{11}NH_2$, DA), 12-Aminolauric acid ($NH_2(CH_2)_{11}COOH$, ALA), and Dodecyl trimethyl ammonium bromide($CH_3(CH_2)_{10}CH_2N(CH_3)_3Br$, DTAB) were selected to represent the natural OM. The selection of the model organics was mainly based on two considerations: the nature of the organics and different mechanisms of OM-clay associations, namely, both interlayer OM-clay complexes synthesized by cation-exchanging (Xi et al., 2007) and OM-clay complexes made by traditional simple mixing (Tannenbaum et al., 1986) were used. These aliphatic organics have similar structures and compounds as some important precursors of oil and gas, such as fatty acids, amino acid, and alkane (Jurg and Eisma, 1964; Liu et al., 1997). In addition, they contain equal lengths of straight-carbon chains but different representative functional groups, which is desirable for the purpose of comparing the pyrolysis mechanisms of these organics. Furthermore, based on the knowledge of intercalation chemistry of clay minerals (Lagaly et al., 2013), both DTAB and DA can be readily cationized and thus can be intercalated into the interlayer of Mt via cation exchange to prepare interlayer clay-OM complexes; ALA is also easily transformed to a protonated amino group ($-NH_3^+$) in acidic solution (Liu et al., 2013); in contrast, intercalation of LA into Mt cannot occur because LA is non-ionic, which allows to compare the interlayer associations and the associations occurring at external surface of Mt.

Thermogravimetry coupled with Fourier transform infrared spectroscopy (TG-FTIR) was used to investigate the pyrolytic behaviors of OM, which is an effective on-line technique to continuously monitor the mass loss of samples during heating and to simultaneously capture compositional information about the corresponding gaseous products in order to highly efficiently detect the mechanisms of pyrolysis.

2. Experiments

2.1. Materials

LA and ALA were supplied by Tokyo Chemical Industry Co., Ltd., DTAB and DA was purchased from Sigma-Aldrich, Co. LLC. These chemical reagents were used without further purification. The raw montmorillonite with the purity of 97% was obtained from Inner Mongolia, China. Before contacted with OM, montmorillonite was sodium modified to get a better swelling property (hereafter labeled as Mt). The chemical compositions (wt%) of Mt are as follows: SiO_2 56.24%, Al_2O_3 14.96%, Fe_2O_3 4.23%, CaO 0.35%, MgO 4.11%, Na_2O 3.13%, K_2O 0.14%, MnO 0.02%, TiO_2 0.31%, P_2O_5 0.03%, and the ignition loss 16.49%. The cationic exchange capacity (CEC) of Mt is 110.50 mmol/100 g.

Two preparation methods, for the complexes where OM exists at the external surface of Mt and for the interlayer complexes, were used. For the former complex, a total of 10 g of Mt sample and 2.5 g of OM were simply mixed and the mixture was ground by ball milling for 20 min using a Pulverisette-6 Planetary Mill. These products were denoted as LA-Mt, DA-Mt, DTAB-Mt, and ALA-Mt, corresponding to the used organics, respectively. The preparation of interlayer OM-Mt complex was performed according to the following procedure. At first, 22.1 mmol ALA were added into 200 mL of 0.14 M HCl solution and kept at 80 °C water bath; then the resultant solution was added into the dispersion composing of 10 g Mt and 1000 mL distilled water to form a mixture; after stirring at 80 °C for 30 min, the solid in the mixture was filtered and repeatedly washed (8 times) with large amounts of hot distilled water, then freeze-dried and ground to powder. The product was labeled as ALA_{inter}-Mt. The preparation of DA_{inter}-Mt and $DTAB_{inter}$-Mt was similar to the above procedure, except the omission of protonation. LA was not used to prepare interlayer OM-Mt complex because it could not be intercalated into the interlayer space of Mt through cation-exchange. All of the above final products were passed through 200 mesh screen for further use except DA-Mt (Because DA melts after grounding, DA-Mt is easy to bind).

2.2. Instruments and methods

The X-ray diffraction (XRD) patterns of samples were recorded on a Bruker D8 Advance diffractometer with Ni filter and CuKα radiation (λ = 0.154 nm) using a generator voltage of 40 kV and a generator current of 40 mA, with a scan rate of 3° (2θ)/min.

The organic content of the interlayer OM-Mt complexes were determined by elemental analysis, which was performed using an Elementar Vario EL III Universal CHNOS elemental analyzer.

The solid acidity of Mt was measured following the methods previously described (Liu et al., 2013). The total amount of solid acid sites of Mt was determined by *n*-butylamine titration using Hammett indicator. The types of solid acid sites (Brønsted acid sites and Lewis acid sites) were differentiated by diffuse reflectance Fourier transform infrared spectroscopy (DRIFT) using pyridine as a probe molecule. The amounts of Brønsted acid sites and Lewis acid sites were also calculated using the method mentioned by Liu et al. (Liu et al., 2011). The detailed detection process and the corresponding results were listed in supplementary material.

The TG-FTIR analysis was conducted on a NETZSCH STA 449C thermal analyzer coupled with a Bruker Vertex-70 Fourier-transform infrared spectrometer. Approximately 10 mg of sample was heated from room temperature to 900 °C at a rate of 20 °C/min in an ultrahigh purity argon flow (40 cm^3/min). After the evolved gases of samples from TG passing through the FTIR cell, absorbance information was obtained at different wavenumber as a function of temperature. The FTIR spectrometer recorded spectra every 13.6 s.

3. Results

3.1. Structural and compositional characteristics of Mt and OM-Mt complexes

The basal reflection of each sample obtained from XRD patterns is listed in Table 1. Compared with Mt (d_{001} = 1.22 nm), no obvious changes of d_{001} values were observed in the (001) reflections of LA-Mt, DA-Mt, and ALA-Mt. This results indicated that intercalation of the related organics did not occur as expected during the preparation, and the organics existed outside of interlayer space of Mt. However, for DTAB-Mt, which showed a d_{001} value of 1.40 nm, implying a small amount of DTAB entered the interlayer of Mt during preparation process. The d_{001} values of DA_{inter}-Mt, ALA_{inter}-Mt, and $DTAB_{inter}$-Mt were 1.74, 1.70, and 1.90 nm, respectively, which indicated a successful intercalation of these OM into the interlayer space of Mt. The content of intercalated DA, ALA, and DTAB in the corresponding interlayer complexes was listed in Table 1.

3.2. TG-FTIR characterization of the pyrolysis of OM-clay complexes

3.2.1. Pyrolytic process of Mt

Two decomposition steps can be observed in the TG curve of Mt (Fig. 1a). The first step occurred below 200 °C with a sharp DTG peak at 114 °C and showed an obvious mass loss of approximately 12.64%, which was attributed to the elimination of external surface-absorbed water (free water) and interlayer water (Bergaya et al., 2006). This attribution was strongly confirmed by the intense signal associated with gaseous water (1300–2000 cm^{-1} and 3500–4000 cm^{-1}) occurred at 114 °C (Fig. 1b and Fig. 1c). The second step in the temperature range of 500 to 700 °C corresponded to the dehydroxylation of the Mt sheets, in which a broad DTG peak was resolved at 628 °C.

3.2.2. Pyrolytic behaviors of OM-clay complexes

Because the OM chosen in this study had the same carbon chain, a summary of the gaseous FTIR characteristic adsorption bands of C—H and their corresponding contributions are listed in Table 2, and aren't described in detail in the following text.

3.2.3. LA and LA-Mt complexes

LA remained stable below 150 °C but decomposed quickly and completely at temperatures ranging from 150 to 300 °C, exhibiting its maximum decomposition rate at 264 °C (Fig. 2a). The corresponding evolved gases of the overall process and the specific temperature at the maximum release rate (264 °C) are shown in Fig. 2b and Fig. 2c, respectively. The occurrence of strong bands at 2934 and 2866 cm^{-1}, as well as bands at 1462 and 1384 cm^{-1}, indicated that the main gaseous products resulting from LA decomposition were aliphatic hydrocarbons. Meanwhile, a considerable amount of carboxylic acid was also identified by the presence of high–intensity bands at 1778 and 3577 cm^{-1} (Pitkänen et al., 1999), and weak bands at 2361 and 2323 cm^{-1} indicated the production of trace amounts of CO_2.

The TG and DTG curves of LA-Mt exhibited the combined characteristics of Mt and LA (Fig. 2d). Two mass loss steps could be identified in the TG curve. The one below 150 °C was ascribed to the elimination of the adsorbed water and interlayer water of Mt, and the corresponding product information was also found in the 3D–FTIR spectrum (Fig. 2e). The mass loss that occurred in the temperature range of 150 to 300 °C was related to the decomposition of LA. The maximum decomposition temperature of LA-Mt was 226 °C, which was approximately 40° C lower than that of LA. This indicated that Mt strongly promoted the thermal degradation of LA. The types of gaseous products of LA-Mt were similar to that of LA, but the ratios of CO_2 to carboxylic acid in these two samples were different (Fig. 2e and Fig. 2c). The carboxyl group of LA mainly decomposed into CO_2 and/or small carboxylic acid molecules. To quantitatively compare the decarboxylation effects of LA in the presence and absence of Mt, the relative areas of the FTIR bands at 2361 and 1778 cm^{-1} of LA and LA-Mt in Fig. 2c were used to evaluate the ratios of CO_2 to carboxylic acid in their gaseous products. This ratio was 0.040 for LA and 0.235 for LA-Mt, which implied that Mt significantly promoted the decarboxylation of LA.

3.2.4. ALA and ALA-Mt complexes

ALA began to decompose after heating at > 200 °C. The major thermal event of ALA occurred in the range of 400 to 550 °C and resulted in a sharp DTG peak at 467 °C (Fig. 3a). The gaseous products at the first step (200–300 °C) were mainly water (Fig. 3b). ALA is similar in terms of structure and functional groups to an amino acid. Intermolecular condensation reactions of amino acids occurs readily and forms water as a product (Li et al., 2008). Thus, it is reasonable to assign the detected water as the product of the condensation reaction of ALA. The major gaseous products at the second step (400–500 °C) were aliphatic hydrocarbon fragments (2930, 2858, 1502, 1459, and 1364 cm^{-1}) (Fig. 3b and Fig. 3c). Minor products, such as CO_2 (2361 cm^{-1}), N–containing compounds (3336 cm^{-1}), and carboxylic acid (3578 and 1777 cm^{-1}), were also identified. The presence of low-intensity bands at 3086 and 912 cm^{-1} indicated the existence of trace

Table 1
The d_{001} values and the total organic content (TOC) of samples.

Samples	LA-Mt	DA_{inter}-Mt	DA-Mt	ALA_{inter}-Mt	ALA-Mt	DTAB-Mt	$DTAB_{inter}$-Mt
d_{001} (nm)	1.29	1.74	1.23	1.70	1.22	1.40	1.90
[a]TOC (wt% sample)	20.00	16.88	20.00	19.00	20.00	20.00	28.38
[b]TOC (mmol/g clay)	1.25	1.10	1.35	1.09	1.16	0.81	1.29

[a] Mass percent content of organic content in sample.
[b] Loading amount of model organic matter of per gram Mt.

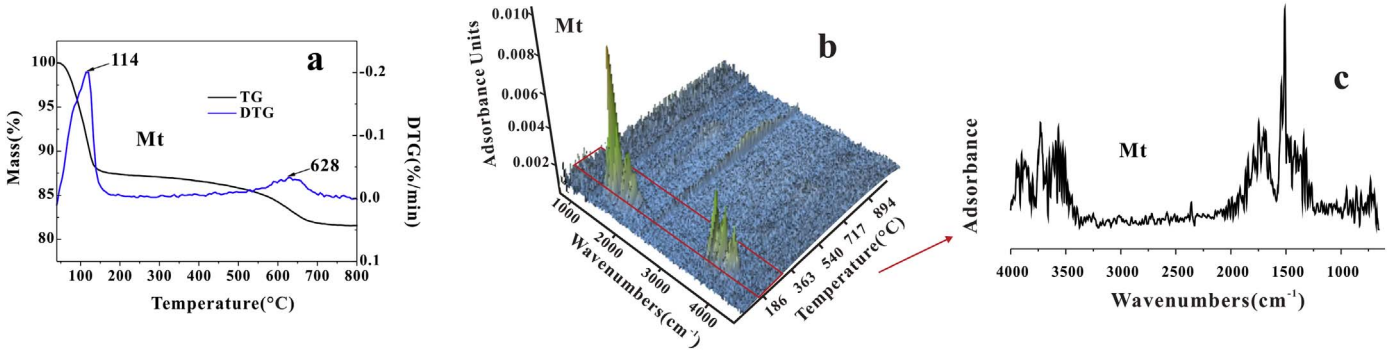

Fig. 1. The TG-FTIR results of Mt: (a) TG-DTG curves; (b) 3D-FTIR spectrum; and (c) FTIR spectrum obtained at the maximum evolution rate.

Table 2
FTIR characteristic adsorption bands of C—H and their corresponding contributions.

Wavenumber (cm^{-1})	Contributions
~3080	=C—H stretching of alkene
~3020	CH_4
~2968	CH_3 stretching
~2934	CH_2 antisymmetrical stretching
~2866	CH_2 symmetrical stretching
~2824	C—H antisymmetrical stretching
~2775	C—H symmetrical stretching
~1462	C—H antisymmetrical bending
~1384	C—H symmetrical bending
~1280	CH_3 rocking

amounts of alkene (Huang and Wang, 2009).

As shown in Fig. 3d and Fig. 3g, the thermal events of ALA-Mt and ALA_{inter}-Mt that occurred below 200 °C were attributed to the dehydration of the adsorbed water and residual interlayer water of Mt, and the mass loss that occurred at the temperature range of 200–500 °C was related to the decomposition of ALA.

For ALA-Mt, most ALA evolved rapidly in the temperature range of 350 to 450 °C, in which a sharp DTG peak was resolved at 402 °C (Fig. 5d). Aliphatic hydrocarbon was the main product, which exhibited strong bands at 2936, 2867, and 1457 cm^{-1} (Fig. 3e and Fig. 3f), accompanied by the formation of a small quantity of NH_3 (965 and 931 cm^{-1}) (Li et al., 2008; Wang et al., 2009). Trace amounts of alkene, CO_2, and carboxylic acids were also released due to the appearance of weak bands at 3018, 2361, and 1779 cm^{-1}, respectively (Marcilla et al., 2005). Small DTG peaks at 235 and 471 °C, which also appeared in the DTG curve of ALA, were attributed to the mass loss of a small amount of ALA, which was unaffected by Mt and decomposed spontaneously.

Two overlapping mass-loss peaks sourced from the degradation of organic matter can be observed at 342 and 372 °C for ALA_{inter}-Mt (Fig. 3g), which were significantly lower than the corresponding temperatures of ALA (by approximately 120 °C). In the temperature range of 200 to 300 °C, the signals of water and CO_2 were detected, indicating that ALA underwent dehydration and decarboxylation processes. Considerable amounts of aliphatic hydrocarbons and NH_3 were formed when the temperature rose from 270 to 500 °C, based on the new

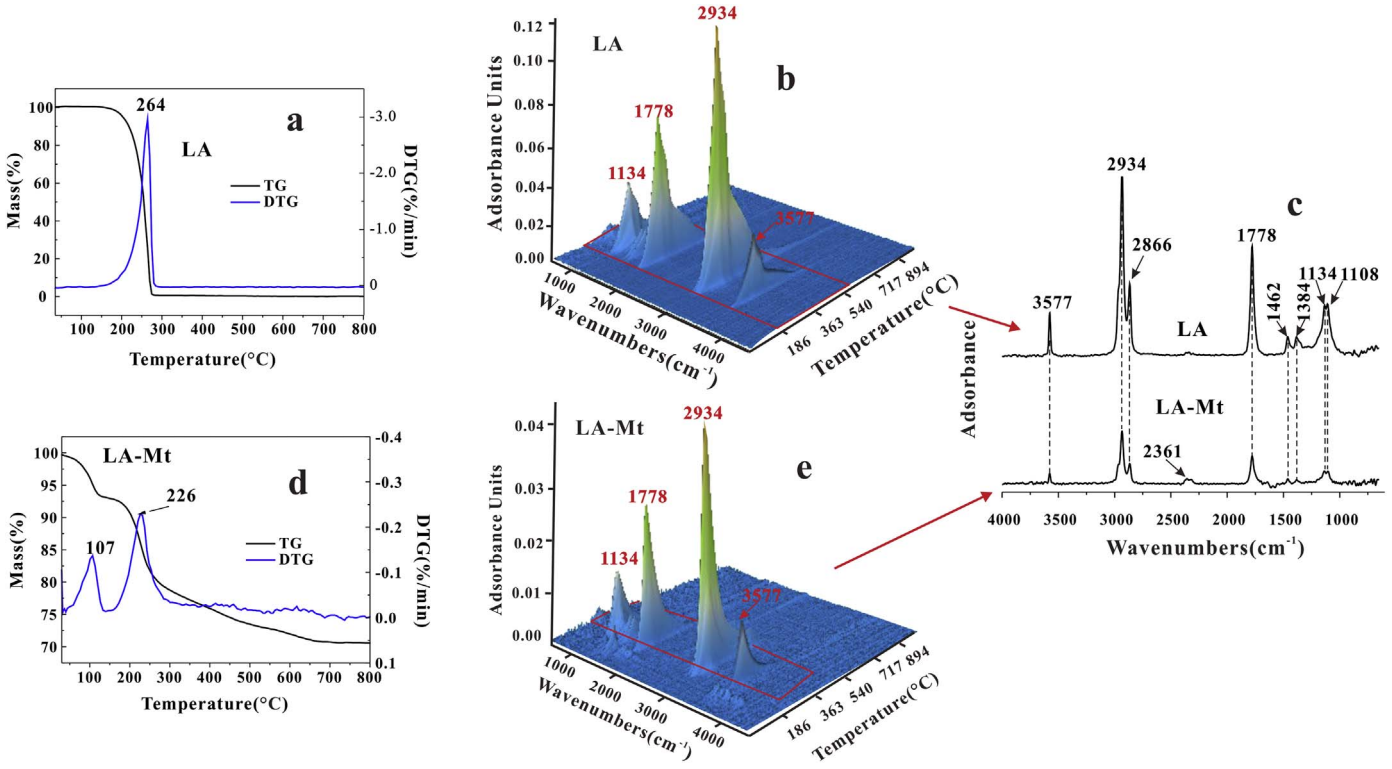

Fig. 2. The TG-FTIR results of LA and LA-Mt: (a and d) TG-DTG curves; (b and e) 3D-FTIR spectra; and (c) FTIR spectra obtained at the maximum evolution rate.

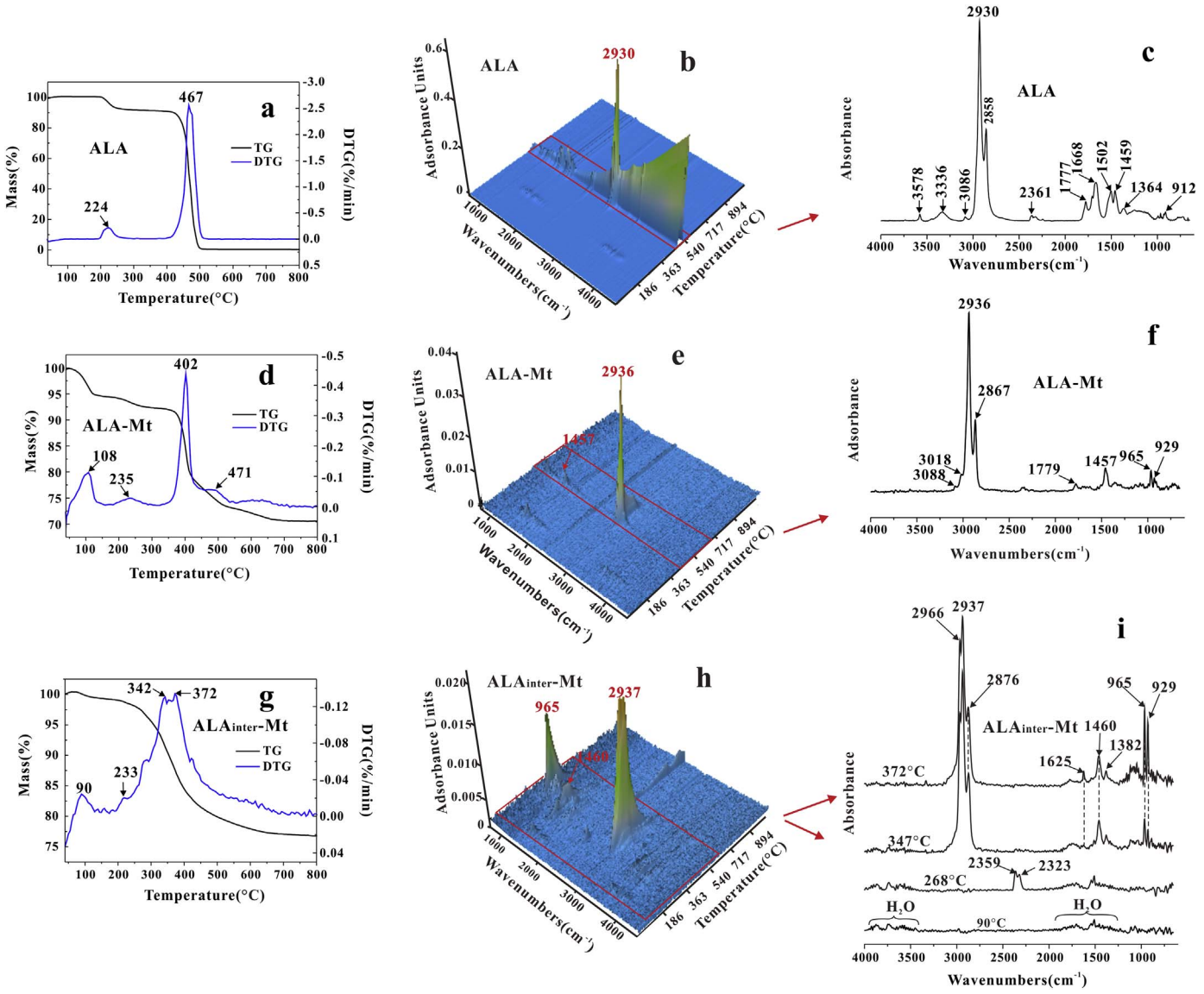

Fig. 3. The TG-FTIR results of ALA, ALA-Mt, and ALA_{inter}-Mt: (a, d, and g) TG-DTG curves; (b, e, and h) 3D-FTIR spectra; and (c, f, and i) FTIR spectra obtained at the maximum evolution rate.

appearance bands of aliphatic hydrocarbons (2966–2876, 1460, and 1382 cm^{-1}) and NH_3 (1625, 966, and 929 cm^{-1}) (Fig. 3h and Fig. 3i). The maximum release rates of hydrocarbons and NH_3 were reached at 347 and 372 °C, respectively. Therefore, the primary reactions that occurred during the decomposition process of ALA_{inter}-Mt were carbon-carbon bond scission and deamination.

3.2.5. DA and DA-Mt complexes

DA decomposed completely below 250 °C, with a strong and sharp DTG peak at 219 °C (Fig. 4a). The main gaseous products of DA were aliphatic hydrocarbons, which showed characteristic bands at 2933, 2865, and 1463 cm^{-1} (Fig. 4b and Fig. 4c). The deviation vibration of N—H (1623 cm^{-1}) and the out-plane bending stretching of N—H (766 cm^{-1}) suggested the presence of a small amount of an unidentified N–containing product. The appearance of these products indicated that DA primarily decomposed via C—C cleavage.

The main decomposition temperature and products of DA-Mt were similar to that of DA (Fig. 4d, Fig. 4e, and Fig. 4c), implying that Mt had almost no effect on the thermal decomposition of DA on the external surface of Mt.

For DA_{inter}-Mt, due to the replacement of interlayer water by DA, the distinct mass loss of the TG curve during the temperature range of 200 to 500 °C was attributed to the pyrolysis of DA. The main DTG peak of DA_{inter}-Mt appeared at 414 °C with a shoulder peak at 315 °C (Fig. 4f), which were both remarkably higher than that of DA (219 °C), indicating that the interlayer space of Mt delayed the thermal decomposition of the DA within it. In other words, the interlayer DA was protected by the sheet of Mt from heating. The main gaseous products released at 315 °C were aliphatic hydrocarbons (2968, 2933, 2870, and 1459 cm^{-1}), accompanied by NH_3 (965 and 931 cm^{-1}) and N–containing compounds (760 cm^{-1}), which were similar to DA and DA-Mt, except for the new appearance of NH_3. As shown in the FTIR spectrum obtained at 409 °C, the band at 760 cm^{-1} disappeared and the signal of HCN at 715 cm^{-1} (Madarász et al., 2004) was detected. Different N-related products indicated that various deamination mechanisms co-existed during the pyrolysis of DA_{inter}-Mt.

3.2.6. DTAB and DTAB-Mt complexes

As shown in Fig. 5, the main DTG peaks of organics in DTAB and DTAB-Mt occurred at similar temperature, i.e., 287 and 292 °C (Fig. 5a and d), respectively, which indicated that the external surface of Mt had little effect on the main pyrolysis temperature of DTAB. The weak DTG

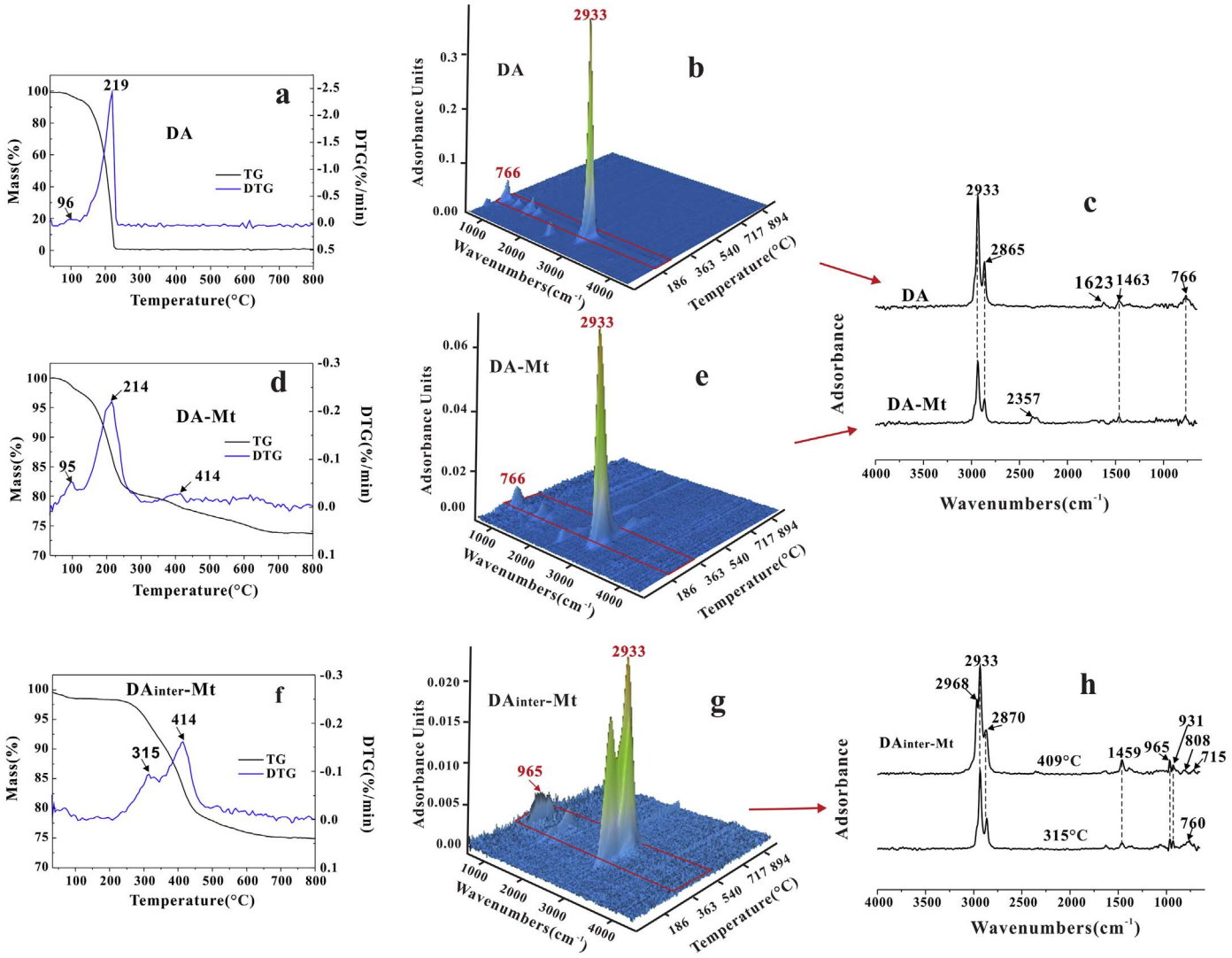

Fig. 4. The TG-FTIR results of DA, DA-Mt, and DA_{inter}-Mt: (a, d, and f) TG-DTG curves; (b, e, and g) 3D-FTIR spectra; and (c and i) FTIR spectra obtained at the maximum evolution rate.

peak of DTAB-Mt at 402 °C indicated that a small amount of DTAB had entered the interlayer space of Mt, which was consistent with the XRD data. The DTG peaks at 307 and 444 °C in $DTAB_{inter}$-Mt, implied that interlayer space greatly delayed the pyrolysis process of DTAB. The gaseous products that evolved from DTAB were mainly aliphatic hydrocarbons. In addition, the bands of CH-stretching (2824 and 2775 cm^{-1}), CH_3-bending (1463 cm^{-1}), CH_3-rocking (1280 cm^{-1}), and CN-stretching (1043 cm^{-1}) confirmed the generation of $(CH_3)_3N$ (trimethylamine) (Suuronen et al., 2002). Similar products were also found in DTAB-Mt and $DTAB_{inter}$-Mt.

4. Discussion

In the absence of Mt, the main pyrolytic processes of OM were rapid, and all gaseous products were released almost simultaneously. As indicated by their products, these OM decomposed mainly via cleavage of C—C bonds. However, for the OM-clay interlayer complexes, the pyrolysis temperature decreased or increased, original single-step reactions became multi-step processes, and the products were also distinct from that of neat OM. In contrast, OM located on the external surface of Mt was mainly affected in terms of its pyrolysis temperature, rather than its products.

4.1. Pyrolysis temperatures of OM in the OM-clay complexes

Mt had contrasting effects on the pyrolysis of different OM, even though all of them were located within the interlayer space of Mt; for example, it promoted ALA and inhibited DA and DTAB (Table 3). To further investigate the pyrolysis process of OM-clay interlayer complexes, three characteristic bands of the main gaseous products of ALA_{inter}-Mt and DA_{inter}-Mt, CO_2 (2359 cm^{-1}), hydrocarbons (2937 cm^{-1}), and NH_3 (965 cm^{-1}), which corresponded to the pyrolysis of –COOH, carbon chain, and $–NH_2$, respectively, were tracked with respect to temperature.

For ALA_{inter}-Mt, the temperatures at which the aforementioned products occurred followed the order: CO_2 (200 °C) < hydrocarbons (250 °C) < NH_3 (270 °C) (Fig. 6a). A similar trend was also found in the maximum release temperatures of these products: CO_2 (268 °C) < hydrocarbons (347 °C) < NH_3 (372 °C), all of which were lower than that of ALA decomposed alone (467 °C). Therefore, the pyrolysis of the $-COOH$, carbon chain, and $-NH_2$ of ALA within the interlayer space of Mt were catalyzed by Mt, and the first decomposition step was decarboxylation, followed by carbon chain cleavage and deamination. For DA_{inter}-Mt, the main production temperature range (250–450 °C) and the maximum release temperature (414 °C) of hydrocarbons and NH_3 were almost the same and higher than that of neat DA, respectively. Meanwhile, the generation of hydrocarbons started at

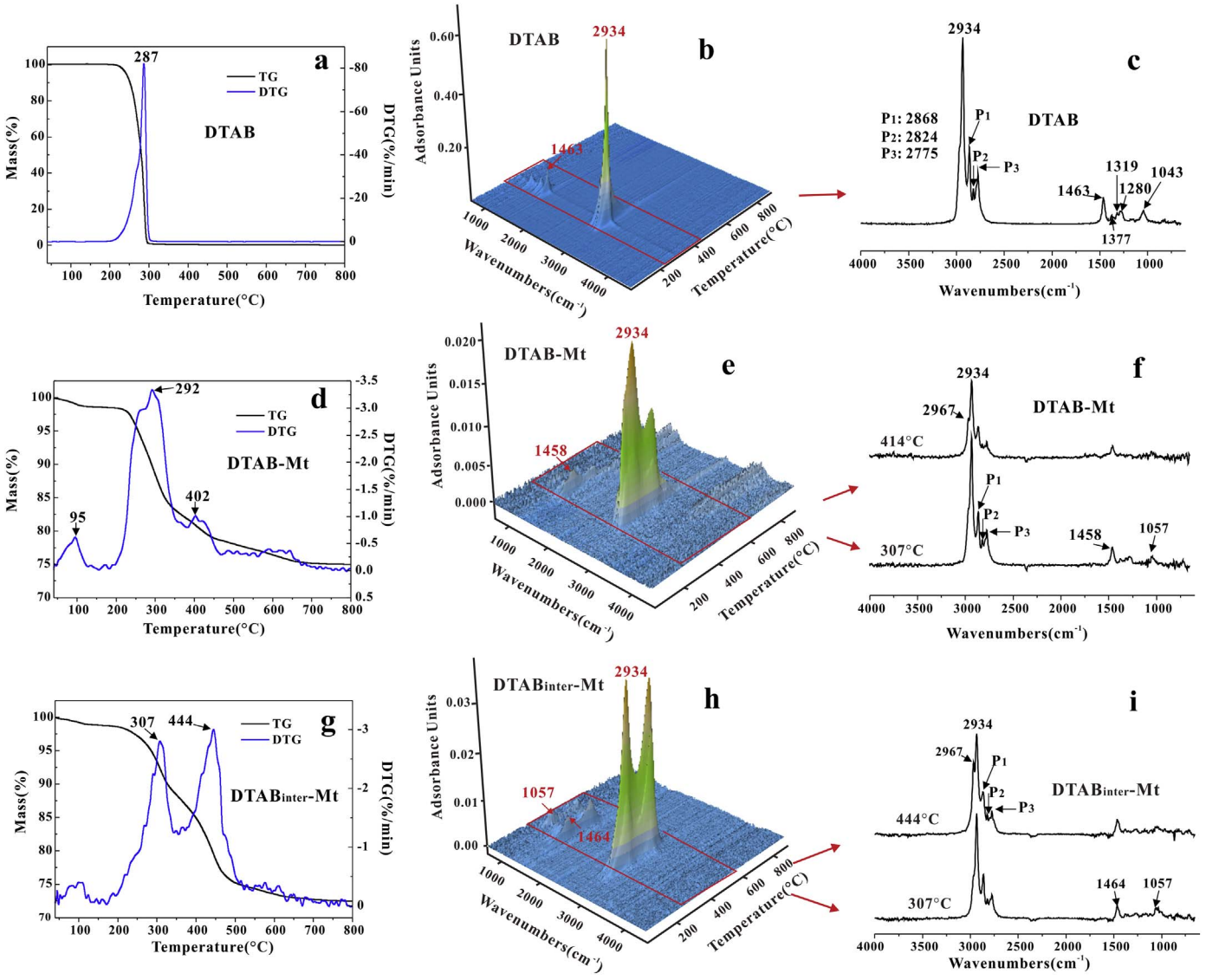

Fig. 5. The TG-FTIR results of DTAB, DTAB-Mt, and $DTAB_{inter}$-Mt: (a, d, and g) TG-DTG curves; (b, e, and h) 3D-FTIR spectra; and (c, f, and i) FTIR spectra obtained at the maximum evolution rate.

Table 3
The main pyrolysis temperature of organics in OM/OM-clay complexes.

Types of OM	Functional groups	OM/OM-clay complex	Main pyrolysis temperature
Fatty acid	−COOH	LA	264
		LA-Mt	226
Amino acid	$-NH_2$	ALA	467
	−COOH	ALA-Mt	402
		ALA_{inter}-Mt	342, 372
Alkylamine	$-NH_2$	DA	219
		DA-Mt	214
		DA_{inter}-Mt	315, 414
Quaternary ammonium salt	$-(CH_3)_3N^+$ Br	DTAB	287
		DTAB-Mt	292
		$DTAB_{inter}$-Mt	307, 444

200 °C, which was 50 °C lower than that of NH_3 (Fig. 6b). Thus, Mt delayed the pyrolysis of the carbon chain and $-NH_2$ of the DA located in the interlayer, and the carbon chain decomposed earlier than $-NH_2$.

The cases of LA-Mt, ALA-Mt, and ALA_{inter}-Mt, clearly indicate that Mt showed a pronounced effect in promoting the pyrolysis of organics with carboxyl groups. Considering the fact that the same functional groups (carbon chain and $-NH_2$) of different interlayer OM (DA and ALA) decomposed at different pyrolysis temperatures and that the carboxyl group was the only structural difference between ALA and DA, it is reasonable to consider that the decarboxylation catalyzed by Mt was the main reason for the acceleration of ALA decomposition, which subsequently induced the occurrence of carbon chain cleavage and deamination in advance.

The pyrolysis temperature of DA and DTAB within the interlayer of Mt was mainly affected by the following factors: 1) The association between OM and clay. The positive charge groups (NH_3^+ and $(CH_3)_3N^+$) of intercalated OM cations adhered tightly to the negative charge-bearing surface site of Mt via electrostatic interaction (Xi et al., 2004), causing the difficulty of decomposition because additional energy was needed to overcome this electrostatic interaction. Thus, their corresponding pyrolysis temperatures were remarkably higher than that of neat OM. 2) The anions associated with the ammonium cations of OM. Ionically bound surfactants (intercalated via cation exchange) were demonstrated to be more thermally stable than unbound free surfactants (which were physically adsorbed by van der Waals forces) with its associated haloid anions (Cui et al., 2008). In essence, haloid anions, such as Br^- and Cl^-, were found to decrease the thermal stability of Quaternary alkyl ammonium-modified clay (Davis et al., 2004;

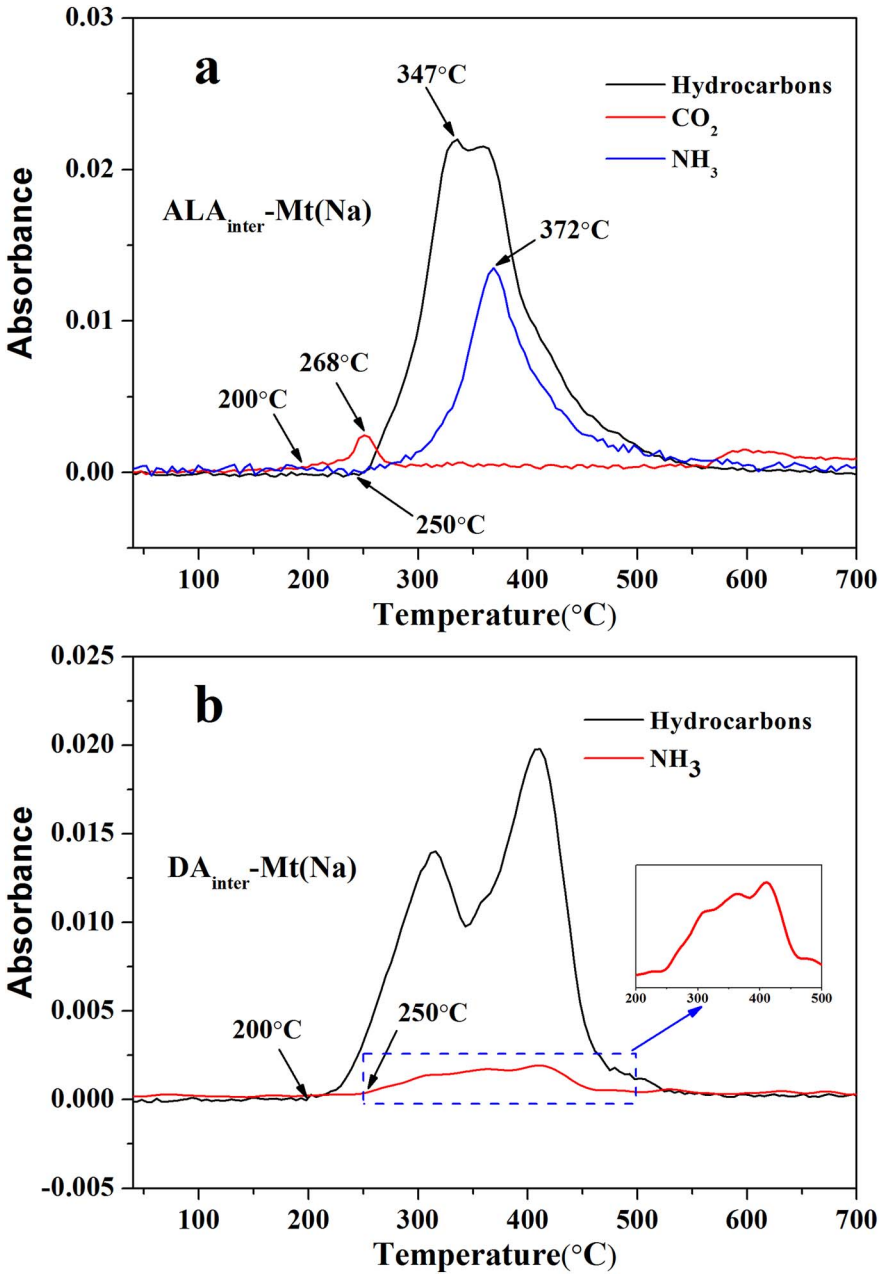

Fig. 6. Distributions of the main gaseous products of ALA_{inter}–Mt and DA_{inter}–Mt with respect to temperature.

Cui et al., 2008).In this study, the loading DTAB within the interlayer space was 1.29 mmol/g, which clearly exceeded the CEC of Mt (1.10 mmol/g), thus reflecting the existence of a considerable amount of unbound DTAB and bromide. Thus, the thermal stability of $DTAB_{inter}$-Mt was inevitably influenced by the residual bromide of these excess unconfined DTAB molecules. 3) The barrier effect of clay mineral sheet. The initial pyrolysis products of interlayer organics were trapped within the confined interlayer spaces and underwent further reactions to produce small-molecular-weight species that were released at a higher temperature (Xie et al., 2001; Bellucci et al., 2007). Thus, the broadness of the temperature range in which the thermal decomposition of intercalated DA occurred and the maximum rate temperature occurred at a higher temperature.

4.2. Pyrolysis mechanism of OM in OM-clay complexes

4.2.1. Fatty acid, amino acid, and alkylamine

4.2.1.1. Decarboxylation mechanism. Decarboxylation was one of the most important reactions of OM with carboxyl groups that occurred in the presence of Mt. Early works agreed that decarboxylation reactions in clay environments involved the transfer of electrons (Almon and Johns, 1975). That is, the Lewis acid sites of clay minerals (the acceptor of electrons pair) catalyzed this decarboxylation. In this study, the amount of Lewis acid sites in Mt reached up to 0.21 mmol/g, which mainly resulted from the octahedral-coordinated Al^{3+} and/or Fe^{3+} cations exposed at the edges of Mt crystallites. In addition, several studies reported that the hydrated cations will become Lewis acid sites after undergoing dehydration (Shimizu et al., 2008). Thus, the residual interlayer cations also exhibited Lewis acidity in high-temperature environments and promoted the generation of CO_2. This part of Lewis acid sites within interlayer space were proposed to account for the distinctly higher yields of CO_2 evolved from ALA_{inter}-Mt than evolved from ALA-Mt.

Although Lewis acid sites are considered to be responsible for decarboxylation, researchers have different opinions on the reaction pathway. Almon and Johns, who investigated the influence of a variety

of layer silicates on the degradation of docosanoic acid, evidenced that Lewis acid sites promoted decarboxylation via a free radical mechanism with the generation of acylate radical intermediates (Almon and Johns, 1975). However, recent theoretical calculation by Geatches et al. (2011) demonstrated the existence of a transition state in the forms of alcohol and CO during the catalytic decarboxylation process of fatty acid to crude oil involving clay minerals. These resulting alcohol intermediates subsequently transformed into hydrocarbons, accompanied by the generation of CO_2 (Geatches et al., 2011). In this study, as the radical intermediates were unstable and hard to detect, and no evidence showed the existence of transition-state products, the decarboxylation pathway might represent one (or both) of the above-mentioned processes.

4.2.1.2. Deamination mechanism. The aliphatic hydrocarbons and NH_3 released during the pyrolysis of ALA_{inter}-Mt, ALA-Mt, and DA_{inter}-Mt suggested the occurrence of Hofmann elimination. Rajagopal et al. previously suggested that the deamination reaction was strongly dependent on the Brønsted acid sites via the Hofmann elimination pathway (Rajagopal et al., 1992). Mt contains abundant Brønsted acid sites, as much as 0.09 mmol/g. These acid sites protonated alkyl amines and initiated the decomposition of them following Hoffmann elimination after heating (Kresnawahjuesa et al., 2002), which produced alkane and NH_3, leaving acidic protons on the surface of Mt caused by β-carbon scission (Leite et al., 2010). A similar phenomenon was also observed in the thermal decomposition of alkylammonium-modified montmorillonite (Xie et al., 2001; Bellucci et al., 2007).

According to the definition of Hoffmann elimination, α-olefins (alkene) was one of the major products. However, unsaturated alkyl products were not found during the pyrolysis of ALA_{inter}-Mt and DA_{inter}-Mt, as they were only detected in the case of ALA-Mt. Reaction sites (i.e., inside or outside interlayers) played a leading role in this conflict. For OM located on the external surface of Mt, its evolved products were transported to the FTIR detector in real time. Nevertheless, for the interlayer OM, its primary products, such as alkene, were confined and had difficulty diffusing due to the steric hindrance of the Mt sheet. With increasing of temperature, the interlayer Brønsted acid sites of Mt catalyzed the hydrogenation reaction of alkene to produce alkane. Protons generated from Hoffmann elimination provided a sufficient H source for this reaction (Fig. 7). Previous pyrolysis studies of kerogen also supported a carbonium ion reaction mechanism involving Brønsted acid sites for the transformation of α-olefins with protons into branched isoalkanes (Pan et al., 2010).

Of particular interest was that the Hoffmann elimination reaction mainly occurred within the interlayer space of Mt, rather than on the external surface. This was related to the source of Brønsted acid sites in Mt. Generally, Brønsted acid sites in Mt result from the polarized water in the interlayer, H_3O^+ adsorbed by the tetrahedral sheet, and the water adsorbed by unsaturated Al^{3+} cations on the edge of the layer (Rupert et al., 1987). In this study, after experiencing high-temperature heating (≥ 300 °C), the surface-adsorbed water of Mt was gone, thus indicating the loss of Brønsted acid sites located on the external surface. However, some of the interlayer water coordinated to cations still existed and exhibited stronger acidity (Frenkel, 1974). Meanwhile, the H_3O^+ that was, adsorbed onto the silicon-oxygen tetrahedral sheet due to electrostatic force, started to produce H^+ and generate new Brønsted acid sites at this temperature (Rupert et al., 1987). That is, in a high-temperature environment, most of the Brønsted acid sites of Mt were sourced from interlayer space, which provided a good opportunity for the OM within interlayers to be catalyzed by these acid sites. Moreover, the protons produced by Hofmann elimination can also act as Brønsted acid sites.

Another interesting phenomenon was that the obviously higher yield but lower maximum release temperature of NH_3 was detected in the case of ALA_{inter}-Mt than that of DA_{inter}-Mt. The $-NH_3^+$ groups of interlayer ALA were attracted by the electrostatic force of the negative-charged surface of Mt. Nevertheless, this positively charged group was also H bonding with a carboxyl group of the other ALA molecules (Huang, 2004). As a result, the C—N bond of ALA was weakened by these two attractive forces from different directions and it was easier to break than that of DA_{inter}-Mt. The observations of ALA-Mt and DA-Mt also supported this inference: a small amount of NH_3 was detected in ALA-Mt, while, this product was absent in the case of DA-Mt. This phenomenon indicated that the coexistence of opposite-charged functional OM groups could affect the pyrolytic behaviors of OM.

4.2.2. Quaternary ammonium salt

The decomposition of ammonium salts has been reported to occur following either a Hoffmann elimination reaction or an S_N2 nucleophilic substitution reaction (Xie et al., 2001). In the former, a Quaternary ammonium salt is decomposed into an olefin, a tertiary amine, and hydrogen chloride or hydrogen bromide in a basic environment (Bellucci et al., 2007; Cope and Trumbull, 2004). In the latter, the nucleophilic attack of neat surfactants by chloride/bromide anions leads to the formation of the free amine and chloromethane/bromomethane (Davis et al., 2004; Cui et al., 2008).

To investigate the pyrolysis mechanism of DTAB and its complexes, a supplementary TG-MS analysis was conducted to monitor the main products related to the above decomposition pathway (see Supplementary material). For neat DTAB, a significantly higher yield of CH_3Br than that of HBr was detected and much more alkane than alkene was also observed (Fig. s1), suggesting that DTAB underwent pyrolysis mainly through S_N2 nucleophilic substitution. Meanwhile, a considerable amount of trimethyl amine was produced slightly later than CH_3Br and HBr. The production of trimethyl amine may result from the second decomposition of the products of bromide-involved elimination or nucleophilic degradation (Davis et al., 2004).

After mixing with Mt, nucleophilic substitution was still the primary pathway for DTAB pyrolysis; however, the elimination reaction was also remarkably enhanced, which was confirmed by the increase of alkene and the increase in the HBr/CH_3Br yield ratio compared to that of neat DTAB (Fig. s2). This enhancement was attributed to the structure and solid acidity of Mt. The Lewis base sites and basic aluminosilicate surface of Mt were conductive to promoting the Hoffmann elimination reaction of the proximal DTAB molecules. Because the external oxygen atoms on the siloxane surface of Mt, which exhibited Lewis basicity (electron donors) (Schoonheydt and Johnston, 2013), can abstract hydrogen from a β-carbon, resulting in the C—N cleavage (Rajagopal et al., 1992). Additionally, as observed in the case of DA and ALA, the Brønsted acid sites of Mt could also catalyze the Hoffmann elimination of DTAB.

For $DTAB_{inter}$-Mt, a strong signal of trimethyl amine was observed

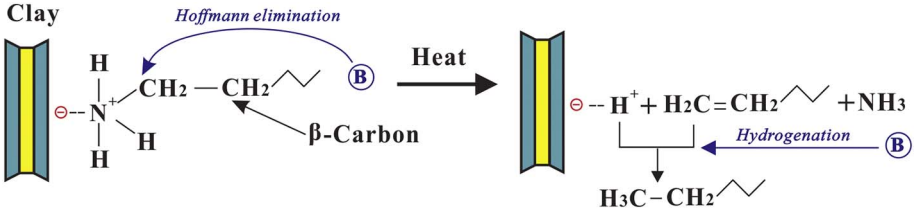

Fig. 7. Proposed Hoffmann elimination and hydrogenation in the pyrolysis of ALA and DA within the interlayer space of Mt.

before the occurrence of HBr and CH_3Br (Fig. s3). Obviously, in contrast to neat DTAB, there was another mechanism for the generation of trimethyl amine. It is probable that the DTAB cations, which entered the interlayer space through cation-exchange and subsequently adhered to the negatively charged surface sites of Mt via electrostatic interaction, underwent Hoffmann elimination via the catalysis of the Brønsted acid sites of Mt and produced trimethyl amine, similar to that which occurred in DA and ALA within the Mt interlayer. The higher yield of HBr than CH_3Br, as well as the higher production of alkene than alkane, further demonstrated that elimination was the main pyrolysis way of $DTAB_{inter}$-Mt. This results agreed well with previous researches (Xie et al., 2001; Davis et al., 2004). Compared with DTAB–Mt, this reverse result was largely attributed to the fact that most Brønsted acid sites were sourced from interlayer space when the temperature exceeded 100 °C (Liu et al., 2011; Liu et al., 2013). Thus, the Brønsted acid sites of Mt were capable of promoting the pyrolysis of DTAB cations and DTAB molecules through Hoffmann elimination.

The above data indicate that the pyrolysis process of OM was significantly affected by the nature of the OM and the association ways between OM and swelling clay minerals (i.e., inside or outside interlayer space). The mechanism by which OM and clay were associated largely depended on the function groups of OM. These groups strongly affected the hydrophobicity, hydrophility, and cation-exchange ability of organics, and they eventually determined whether or not organics could enter the interlayer space of swelling clay minerals. In addition, these functional groups played an important role in determining the thermal stability of OM-clay complexes, such as carboxyl groups and halide anions. The effects of these associations on the pyrolytic behavior of OM were closely related to the properties and structures of clay minerals. For example, attractive forces arose from clay mineral sheet with negative charges and the steric effects of clay mineral sheet affected the onset and maximum release temperature of pyrolytic products. Additionally, the solid acidity, including the structural source (interlayer or external), types (Brønsted acid sites or Lewis acid sites), and the amount of solid acid sites, influenced the pyrolysis pathway and reaction intensity of OM.

4.3. Implications for the transformation of OM-clay complexes in natural environments

The present results indicate that montmorillonite successively accelerated the decarboxylation, C—C bond cleavage, and deamination of fatty acid and amino acid with moderate carbon-chains. The degradation mechanism of these OM complexed with clay was in good agreement with field observations. On the one hand, during progressive sedimentary burial, the O/C ratios decreased with the maturation of organic matter (Vandenbroucke and Largeau, 2007), and the maximum release peak of CO_2 was shallower than the “oil window” (Seewald, 2003). On the other hand, abundant nitrogen was released in the form of NH_3 accompanied by the thermal evolution process of organics (Cooper and Abedin, 1981; Cooper and Raabe, 1982; Williams and Ferrell Jr, 1991; Williams et al., 1992). Thus, our study provided one of the deoxidation and deamination pathways involving clay minerals during the evolution of oxygen- and nitrogen-containing organics.

The decarboxylation of fatty acid and subsequent cracking were proposed to be two important reactions during petroleum generation (Jurg and Eisma, 1964; Shimoyama and Johns, 1971), and amino acids were considered to be potential hydrocarbon sources after deamination and decarboxylation. Thus, fatty acids and amino acids were regarded as two kinds of important sedimentary organic matter for immaturate/low-maturity source rock with a shallow burial depth (Shi et al., 1995; Liu et al., 1997; Shi and Xiang, 2001; Li et al., 2003). Thus, given that most swelling clay minerals (mainly montmorillonite and illite/montmorillonite) are distributed at the shallow depth (Merriman, 2005), the present pyrolysis mechanism of fatty acid and amino acid in the presence of clay was particularly applicable to the study of formation mechanism of bio-thermocatalytic transitional-zone gas involving the catalysis of swelling clay. This proposal was supported by the analysis of the catalysis of clay minerals on the pyrolysis of kerogen extracted from the transitional zone source, in which montmorillonite was found to be the major catalyst in the formation of the transitional-zone gas, because it increased the gas production of organic matter and reduced the thermo-degraded temperature by 50 °C (Lei et al., 1997).

In addition to the aforementioned catalysis effect, the delaying or protecting effect of clay for some clay-OM complexes (e.g., DA/DTAB-Mt interlayer complexes) was also observed. This phenomenon not only implied the complexity of OM pyrolysis in clay-rich source rock but also demonstrated the importance of microstructures of clay and the nature of OM in the preservation and pyrolysis of OM. Abundant studies have indicated that swelling clay minerals act as excellent natural adsorbents for OM in sediments due to their active structural sites, such as exchangeable cations, hydrophobic surfaces and Si-OH (Cornejo et al., 2008). Soluble organics can interact with these active sites to form organic-clay external/interlayer complexes (Lagaly et al., 2013). These associations are not only conducive to the accumulation of OM but also protect them from bio-degradation. In this study, the analysis of halide-containing organics also implied that the thermal stability of related organics was affected by halide anions and that the primary pyrolysis mechanism mostly depended on the relative amounts of halide anions and Brønsted acid sites of the clay minerals of the microenvironment. Recent research also found that Mt had an inhibiting effect on the pyrolysis of halide-containing organics in a confined gold capsule system (Bu et al., 2017). Therefore, the nature of OM, the structure and solid acidity of clay minerals, and the complexation mechanism between OM and clay minerals must be considered together when evaluating the hydrocarbon-generation potential of natural organics in argillaceous source rocks.

The present experiment further verified the significance of swelling clay minerals in the storage and pyrolysis of OM. Swelling clay mineral has a large inner surface area due to its interlayer space, which provides considerable space for the storage of organics. Rich organic resources are the physical basis of oil and gas reservoirs. Thus, abundant swelling clay minerals in sediment can be considered to be a good precondition for great oil and gas potential. Furthermore, as described earlier, Mt exhibited much more distinct catalysis or delaying effects for OM existing in interlayer space rather than that in external sites, which was primarily attributed to the abundance of interlayer solid acid sites, especially Brønsted acid sites. Due to the extensive existence of swelling clays and the wide occurrence of OM-clay (swelling clay) complexes in geological environments, the role of swelling clay minerals during diagenesis deserves more attention.

5. Conclusions

In this work, the pyrolysis of organic matter with different functional groups occurring in and out of Mt interlayer was studied. Mt had significant effects on the pyrolytic temperature and products of OM. Different effects of Mt on the pyrolytic temperature were observed in different OM, i.e., it accelerated LA and ALA pyrolysis but delayed DA and DTAB pyrolysis. Mt also changed the products of pyrolysis, by promoting the decarboxylation and Hoffmann elimination of these OM. The evolution of carboxyl groups under the catalysis of Mt accounted for the decrease in the decomposition temperature of carboxyl group-containing OM.

All of these results indicated that interlayer space might be a more important than external surface of Mt for promoting or delaying the pyrolysis of organic matter due to the abundance of interlayer solid acid sites and the negative charge and steric hindrance of clay layers. The Lewis acid sites of Mt were responsible for the decarboxylation of organics. The Brønsted acid sites of Mt were capable of promoting the pyrolysis of nitrogen-containing organics through Hoffmann elimination. Brønsted acid sites of clay minerals and halide anions were crucial

factors in determining the thermal stability and pyrolysis pathway of the halide-containing organic-clay complexes. The case of ALA implied that the coexistence of opposite-charged functional groups of OM could affect the pyrolytic behaviors of OM.

The findings of this work clearly demonstrated that the pyrolysis process of OM in the presence of clay minerals strongly depended on the nature of OM, the nature of clay minerals, and the association ways between organics and clay minerals.

Acknowledgments

This work was financially supported by the National Natural Science Foundation of China (Grant No. 41502031, 41272059, 41472044, and 41673066), Science Foundation of Guangdong Province, China (Grant No. 2015A030310363 and 2014A030313682), Science and Technology Program of Guangzhou, China (Grant No. 201607010280 and 201510010153), and the Youth Innovation Promotion Association of CAS. This is contribution No.IS-2480 from GIGCAS.

Appendix A. Supplementary data

Supplementary data to this article can be found online at https://doi.org/10.1016/j.clay.2017.12.028.

References

Almon, W., Johns, W., 1975. Petroleum forming reactions: the mechanism and rate of clay catalyzed fatty acid decarboxylation. Advances in. Org. Geochem. 157–172.
Bellucci, F., Camino, G., Frache, A., Sarra, A., 2007. Catalytic charring–volatilization competition in organoclay nanocomposites. Polym. Degrad. Stab. 92 (3), 425–436.
Bergamaschi, B.A., Tsamakis, E., Keil, R.G., Eglinton, T.I., Montluçon, D.B., Hedges, J.I., 1997. The effect of grain size and surface area on organic matter, lignin and carbohydrate concentration, and molecular compositions in Peru Margin sediments. Geochim. Cosmochim. Ac. 61 (6), 1247–1260.
Bergaya, F., Theng, B.K.G., Lagaly, G., 2006. Handbook of Clay Science. vol. 1 Elsevier Science.
Bu, H., Yuan, P., Liu, H., Liu, D., Liu, J., He, H., Zhou, J., Song, H., Li, Z., 2017. Effects of complexation between organic matter (OM) and clay mineral on OM pyrolysis. Geochim. Cosmochim. Ac. 212, 1–15.
Cai, J., Bao, Y., Yang, S., Wang, X., Fan, D., Xu, J., Wang, A., 2007. Research on preservation and enrichment mechanisms of organic matter in muddy sediment and mudstone. Sci. China Ser. D Earth Sci. 50 (5), 765–775.
Cooper, J.E., Abedin, K.Z., 1981. The relationship between fixed ammounium-nitrogen and postassium in clay from a deep well on the Texas Gult-Coast. Tex. J. Sci. 33 (2–4), 103–111.
Cooper, J.E., Raabe, B.A., 1982. The effect of thermal gradient on the distribution of nitrogen in a shale. Tex. J. Sci. 34 (2), 175–182.
Cope, A.C., Trumbull, E.R., 2004. Olefins from amines: the hofmann elimination reaction and amine oxide pyrolysis. In: Organic Reactions. John Wiley & Sons, Inc..
Cornejo, J., Celis, R., Pavlovic, I., Ulibarri, M.A., 2008. Interactions of pesticides with clays and layered double hydroxides: a review. Clay Miner. 43 (2), 155.
Cui, L., Hunter, D.L., Yoon, P.J., Paul, D.R., 2008. Effect of organoclay purity and degradation on nanocomposite performance, part 2: morphology and properties of nanocomposites. Polymer 49 (17), 3762–3769.
Davis, R., Gilman, J., Sutto, T., Callahan, H.J., Trulove, P., De Long, H., 2004. Improved thermal stability of organically modified layered silicates. Clay Clay Miner. 52 (2), 171–179.
Faure, P., Schlepp, L., Burkle-Vitzthum, V., Elie, M., 2003. Low temperature air oxidation of n-alkanes in the presence of Na-smectite. Fuel 82 (14), 1751–1762.
Faure, P., Jeanneau, L., Lannuzel, F., 2006. Analysis of organic matter by flash pyrolysis-gas chromatography–mass spectrometry in the presence of Na-smectite: when clay minerals lead to identical molecular signature. Org. Geochem. 37 (12), 1900–1912.
Frenkel, M., 1974. Surface acidity of montmorillonites. Clay Clay Miner. 22 (5–6), 435–441.
Geatches, D., Greenwell, C., Clark, J.S., 2011. Ab initio transition state searching in complex systems: fatty acid decarboxylation in minerals. J. Phys. Chem. C 115, 2658–2667.
He, H., Ding, Z., Zhu, J., Yuan, P., Xi, Y., Yang, D., Frost, R.L., 2005. Thermal characterization of surfactant-modified montmorillonits. Clay Clay Miner. 53 (3), 287–293.
Heller-Kallai, L., Aizenshtat, Z., Miloslavski, I., 1984. The effect of various clay minerals on the thermal decomposition of stearic acid under “bulk flow” conditions. Clay Miner. 19 (5), 779–788.
Huang, P.M., 2004. Soil mineral–organic matter—microorganism interactions: fundamentals and impacts. Adv. Agron. 82, 391–472.
Huang, N., Wang, J., 2009. A TGA-FTIR study on the effect of $CaCO_3$ on the thermal degradation of EBA copolymer. J. Anal. Appl. Pyrolysis 84 (2), 124–130.
Ingalls, A.E., Aller, R.C., Lee, C., Wakeham, S.G., 2004. Organic matter diagenesis in shallow water carbonate sediments. Geochim. Cosmochim. Ac. 68 (21), 4363–4379.
Jurg, J., Eisma, E., 1964. Petroleum hydrocarbons: generation from fatty acid. Science 144 (3625), 1451.
Keil, R.G., Tsamakis, E., Fuh, C.B., Giddings, J.C., Hedges, J.I., 1994. Mineralogical and textural controls on the organic composition of coastal marine sediments: hydrodynamic separation using SPLITT-fractionation. Geochim. Cosmochim. Ac. 58 (2), 879–893.
Kennedy, M.J., Wagner, T., 2011. Clay mineral continental amplifier for marine carbon sequestration in a greenhouse ocean. P. Natl. Acad. Sci. Usa. 108 (24), 9776–9781.
Kennedy, M.J., Pevear, D.R., Hill, R.J., 2002. Mineral surface control of organic carbon in black shale. Science 295 (5555), 657–660.
Kennedy, M.J., Löhr, S.C., Fraser, S.A., Baruch, E.T., 2014. Direct evidence for organic carbon preservation as clay-organic nanocomposites in a Devonian black shale; from deposition to diagenesis. Earth Planet. Sc. Lett. 388, 59–70.
Kresnawahjuesa, O., Gorte, R., de Oliveira, D., Lau, L., 2002. A simple, inexpensive, and reliable method for measuring Brønsted-acid site densities in solid acids. Catal. Lett. 82 (3–4), 155–160.
Lagaly, G., Ogawa, M., Dékány, I., 2013. Chapter 10.3 - clay mineral–organic interactions. In: Bergaya, F., Lagaly, G. (Eds.), Developments in Clay Science. Elsevier.
Lei, H., Shi, Y., Guan, P., Fang, X., 1997. Catalysis of aluminosilicate clay minerals to the formation of the transitional zone gas. Sci. China Ser. D 40 (2), 130–136.
Leite, I.F., Soares, A.P.S., Carvalho, L.H., Raposo, C.M., Malta, O.M., Silva, S.M., 2010. Characterization of pristine and purified organobentonites. J. Therm. Anal. Calorim. 100 (2), 563–569.
Li, Z., Zhang, Z.L., Sun, Y.H., Lao, Y.X., Lin, W.Z., Wu, W.F., 2003. Catalytic decarboxylations of fatty acids in immature oil source rocks. Sci. China Ser. D 46 (12), 1250–1260.
Li, J., Liu, Y., Shi, J., Wang, Z., Hu, L., Yang, X., Wang, C., 2008. The investigation of thermal decomposition pathways of phenylalanine and tyrosine by TG–FTIR. Thermochim. Acta 467 (1–2), 20–29.
Liu, W.H., Xu, Y.C., Shi, J.Y., Lei, H.Y., Zhang, B.S., 1997. Evolution model and formation mechanism of bio-thermocatalytic transitional zone gas. Sci. China Ser. D 40 (1), 43–53.
Liu, D., Yuan, P., Liu, H.M., Cai, J.G., Qin, Z.H., Tan, D.Y., Zhou, Q., He, H.P., Zhu, J.X., 2011. Influence of heating on the solid acidity of montmorillonite: a combined study by DRIFT and Hammett indicators. Appl. Clay Sci. 52 (4), 358–363.
Liu, H.M., Liu, D., Yuan, P., Tan, D.Y., Cai, J., He, H.P., Zhu, J.X., Song, Z.G., 2013. Studies on the solid acidity of heated and cation-exchanged montmorillonite using *n*-butylamine titration in non-aqueous system and diffuse reflectance Fourier transform infrared (DRIFT) spectroscopy. Phys. Chem. Miner. 40 (6), 479–489.
Lopez-Sangil, L., Rovira, P., 2013. Sequential chemical extractions of the mineral-associated soil organic matter: an integrated approach for the fractionation of organo-mineral complexes. Soil Biol. Biochem. 62, 57–67.
Lu, X.C., Hu, W.X., Fu, Q., Miao, D.Y., Zhou, G.J., Hong, Z.H., 1999. Study of combination pattern of soluble organic matters and clay minerals in the immature source rocks in Dongying depression, China. Chinese J. Geol. 34 (1), 69–77.
Madarász, J., Krunks, M., Niinistö, L., Pokol, G., 2004. Evolved gas analysis of dichlorobis (thiourea)zinc(II) by coupled TG-FTIR and TG/DTA-MS techniques. J. Therm. Anal. Calorim. 78, 679–686.
Marcilla, A., Gómez, A., Menargues, S., 2005. TGA/FTIR study of the catalytic pyrolysis of ethylene–vinyl acetate copolymers in the presence of MCM-41. Polym. Degrad. Stab. 89 (1), 145–152.
Mayer, L.M., 1994. Surface area control of organic carbon accumulation in continental shelf sediments. Geochim. Cosmochim. Ac. 58 (4), 1271–1284.
Mayer, L.M., 1999. Extent of coverage of mineral surfaces by organic matter in marine sediments. Geochim. Cosmochim. Ac. 63 (2), 207–215.
Mayer, L.M., 2004. The inertness of being organic. Mar. Chem. 92 (1–4), 135–140.
Merriman, R.J., 2005. Clay minerals and sedimentary basin history. Eur. J. Mineral. 17 (1), 7–20.
Pan, C.C., Jiang, L.L., Liu, J.Z., Zhang, S.C., Zhu, G.Y., 2010. The effects of calcite and montmorillonite on oil cracking in confined pyrolysis experiments. Org. Geochem. 41 (7), 611–626.
Perezrodriguez, J.L., Weiss, A., Lagaly, G., 1977. Natural clay organic complex from Andalusian black earth. Clay Clay Miner. 25 (3), 243–251.
Pitkänen, I., Huttunen, J., Halttunen, H., Vesterinen, R., 1999. Evolved gas analysis of some solid fuels by TG-FTIR. J. Therm. Anal. Calorim. 56 (3), 1253–1259.
Rajagopal, S., Grimm, T.L., Collins, D.J., Miranda, R., 1992. Denitrogenation of piperidine on alumina, silica, and silica-aluminas: the effect of surface acidity. J. Catal. 137 (2), 453–461.
Ransom, B., Kim, D., Kastner, M., Wainwright, S., 1998. Organic matter preservation on continental slopes importance of mineralogy and surface area. Geochim. Cosmochim. Ac. 62 (8), 1329–1345.
Rupert, J.P., Granquist, W.T., Pinnavaia, T.J., 1987. Catalytic properties of clay minerals. In: Newman, A.C.D. (Ed.), Chemistry of Clays and Clay Minerals. Longman scientific and technical, New York.
Schoonheydt, R.A., Johnston, C.T., 2013. Chapter 5 - surface and interface chemistry of clay minerals. In: Bergaya, F., Lagaly, G. (Eds.), Developments in Clay Science. Elsevier.
Schulten, H.R., Leinweber, P., Theng, B.K.G., 1996. Characterization of organic matter in an interlayer clay-organic complex from soil by pyrolysis methylation-mass spectrometry. Geoderma 69 (1–2), 105–118.
Seewald, J.S., 2003. Organic–inorganic interactions in petroleum-producing sedimentary basins. Nature 426 (6964), 327–333.
Shi, J., Xiang, M., 2001. The occurrence of fatty acids in immature source rocks and their distribution characteristics. Chin. Sci. Bull. 46 (2), 166–170.
Shi, J., Xiang, M., Qu, D., Zhou, Y., 1995. Significance of amino acids and fatty acids for the formation of the bio-thermocatalytic transition zone gases. Acta Sedimentol. Sin.

13 (2), 33–43.
Shimizu, K.-I., Higuchi, T., Takasugi, E., Hatamachi, T., Kodama, T., Satsuma, A., 2008. Characterization of Lewis acidity of cation-exchanged montmorillonite K-10 clay as effective heterogeneous catalyst for acetylation of alcohol. J. Mol. Catal. A Chem. 284 (1–2), 89–96.
Shimoyama, A., Johns, W.D., 1971. Catalytic conversion of fatty acids to petroleum-like paraffins and their maturation. Nature 232 (33), 140–144.
Suuronen, J., Pitkänen, I., Halttunen, H., Moilanen, R., 2002. Formation of the main gas compounds during thermal analysis and pyrolysis: betaine and betaine monohydrate. J. Therm. Anal. Calorim. 69 (1), 359–369.
Tannenbaum, E., Huizinga, B., Kaplan, I., 1986. Role of minerals in thermal alteration of organic matter. II- a material balance. AAPG Bull. 70, 1156–1165.
Theng, B.K.G. (Ed.), 1974. The Chemistry of Clay-Organic Reactions. Adam Hilger, London.
Theng, B.K.G., Churchman, G.J., Newman, R.H., 1986. The occurrence of interlayer clay-organic complexes in two New Zealand soils. Soil Sci. 142 (5), 262–266.
Vandenbroucke, M., Largeau, C., 2007. Kerogen origin, evolution and structure. Org. Geochem. 38 (5), 719–833.
Wang, M.C., Huang, P.M., 1986. Humic macromolecule interlayering in nontronite through interaction with phenol monomers. Nature 323 (6088), 529–531.
Wang, Z., Lv, P., Hu, Y., Hu, K., 2009. Thermal degradation study of intumescent flame retardants by TG and FTIR: melamine phosphate and its mixture with pentaerythritol. J. Anal. Appl. Pyrolysis 86 (1), 207–214.
Williams, L.B., Ferrell Jr., R., 1991. Ammonium substitution in illite during maturation of organic matter. Clay Clay Miner. 39 (4), 400–408.
Williams, L.B., Wilcoxon, B.R., Ferrell, R.E., Sassen, R., 1992. Diagenesis of ammonium during hydrocarbon maturation and migration, Wilcox Group, Louisiana, U.S.A. Appl. Geochem. 7 (2), 123–134.
Xi, Y., Ding, Z., He, H., Frost, R.L., 2004. Structure of organoclays—an X-ray diffraction and thermogravimetric analysis study. J. Colloid Interface Sci. 277 (1), 116–120.
Xi, Y., Frost, R.L., He, H., 2007. Modification of the surfaces of Wyoming montmorillonite by the cationic surfactants alkyl trimethyl, dialkyl dimethyl, and trialkyl methyl ammonium bromides. J. Colloid Interface Sci. 305 (1), 150–158.
Xie, W., Gao, Z., Pan, W.-P., Hunter, D., Singh, A., Vaia, R., 2001. Thermal degradation chemistry of alkyl quaternary ammonium montmorillonite. Chem. Mater. 13 (9), 2979–2990.
Yu, W.H., Li, N., Tong, D.S., Zhou, C.H., Lin, C.X., Xu, C.Y., 2013. Adsorption of proteins and nucleic acids on clay minerals and their interactions: a review. Appl. Clay Sci. 80–81, 443–452.
Zhang, Z.L., Ren, Y., Yan, Z., Zhang, T., 2005. Kinetics on hydrocarbon generation from fatty acid ester in the presence of natural minerals at low temperature. Geochimica 34 (3), 263–268.
Zhu, J.X., Zhu, L.Z., Zhu, R.L., Tian, S.L., Li, J.W., 2009. Surface microtopography of surfactant modified montmorillonite. Appl. Clay Sci. 45 (1–2), 70–75.
Zhu, X., Cai, J.G., Liu, W., Lu, X., 2016. Occurrence of stable and mobile organic matter in the clay-sized fraction of shale: significance for petroleum geology and carbon cycle. Int. J. Coal Geol. 160-161, 1–10.